Toll-like receptor-mediated IRE1α activation as a therapeutic target for inflammatory arthritis

Quan Qiu[1], Ze Zheng[2], Lin Chang[9], Yuan-Si Zhao[3], Can Tan[1], Aditya Dandekar[5], Jenney Z. Zhang[4], Zhenghong Lin[1], Ming Gui[1], Xiu Li[7] , Tongshuai Zhang[7], Qingfei Kong[1,7], Hulun Li[7], Sha Chen[8], An Chen[8], Randal J. Kaufman[10], William Yang[11], Hui-Kuan Lin[11], Donna Zhang[12], Harris Perlman[12], Edward Thorp[1], Kezhong Zhang[2,5 #] and Deyu Fang[1,4 #]

Supplemental files:

1. Supplemental Materials & Methods
2. Supplemental Table 1
3. Supplemental figures 1-15 and their legends.
4. **Unprocessed images of all figures and supplemental figures.**

Supplemental Materials and Methods (Qiu et al)

Cells and Reagents. Human endothelial kidney (HEK) 293 cells were maintained in Dulbecco's Modification of Eagle's Medium (Cellgro, Mediatech, MA, USA) containing 10% fetal calf serum (GIBCO, Invitrogen, Grand Island, NE, USA). Transfection in HEK 293T cells was performed with Lipofectamine™ 2000 protocol (Invitrogen, Grand Island, NE, USA). Mouse RAW 264.7 cells were also cultured in 10% FCS-containing D-MEM. Wild-type and TRAF6 knockout MEF cells were cultured as previously reported (Yang et al, 2009). Plasmids expressing IRE1α and its truncated mutants were generated by PCR using linker primers and sub-cloned into pCMV-Flag vector (Sigma-Aldrich, St. Louis, MO, USA). Myc-tagged TRAF6 expression plasmid and its C70A mutant were used as reported (Yang et al, 2009). The truncated mutants were generated by PCR with linker primers followed by sub-cloning into pCMV-Myc vector (Invitrogen, Grand Island, NE, USA). lipopolysaccharide (LPS) and polyinosinic–polycytidylic acid potassium salt (poly(I:C)) were purchased from Sigma-Aldrich. Tripalmitoyl cysteinyl seryl tetralysine lipopeptide (Pam3CSK4) was purchased from InvivoGen (San Diego, CA, USA). Tunicamycin was purchased from Enzo (Farmingdale, USA). The resources of antibodies are as the following: IRE1α, phosph-eIF2α (Cell Signaling, Danvers, MA, USA); ATF6 (abcam, Cambridge, MA, USA); Flag, β-actin, and Tubulin (Sigma-Aldrich); c-Myc and HA (Santa Cruz Biotech, Santa Cruz, CA, USA); TRAF6 (Prosci, Poway, CA USA); PP2A (BD Bioscience, San Diego, CA, USA) and all the antibodies against the cell surface molecules for flow cytometry (Biolegend, San Diego, CA, USA). The IRE1α inhibitor 4U8C was purchased from Ryan Scientific (Mount Pleasant, SC, USA).

Isolation of RNA from human synovial macrophages. Synovial fluids from RA and OA patients were cultivated in the 6-well plate for 2 hours. Adherent cells were collected and lyszed by Trizol and the total RNA was isolated.

Mice. The *IRE1α^flox/flox* mice were generated as previously described [29]. The *IRE1α^flox/flox* mice were backcrossed with C57BL/6J mice for over 10 generations to maintain the C57BL strain background. The myeloid-specific *IRE1α* knockout mice were generated by crossing *IRE1α^flox/flox* mice with transgenic mice expressing *Cre* under the control of the *lysozyme M* (*LysM*) gene promoter (LysM-Cre). *LysM*-Cre transgenic mice were purchased from Jackson laboratory. All mice used in this study were maintained and used at the Northwestern University mouse facility under pathogen-free conditions according to

institutional guidelines and animal study proposals approved by the institutional animal care and use committees.

Transfection, co-immunoprecipitation and western blotting analysis. Transient transfection of HEK 293T cells was performed by using Lipofectamine 2000 (Invitrogen), according to the manufacturer's instructions. Two days after transfection, cells were lysed in Nonidet P-40 lysis buffer (1%Nonidet P-40, 20 mM Tris-HCl, pH 7.5, 150 mM NaCl, 5 mM EDTA, and freshly added protease inhibitor cocktails). The cell lysates were incubated with an antibody (1 µg) for 2 hr on ice, followed by the addition of 30 µL of fast-flow protein G-Sepharose beads (GE Healthcare Bioscience, Uppsala, Sweden) overnight at 4 °C. Immunoprecipitates were washed four times with NP-40 lysis buffer and boiled in 30 µL of 2× Laemmli buffer. Samples were subjected to 8% or 10% SDS-PAGE analysis and electrotransferred onto nitrocellulose membranes (0.45µM; Bio-Rad). Membranes were probed with the indicated primary antibodies, followed by horseradish peroxidase-conjugated secondary antibodies. Membranes were then washed and visualized with an enhanced chemiluminescence detection system (Bio-Rad, Hercules, CA, USA). When necessary membranes were stripped by incubation in stripping buffer (Thermo, Rockford, MA, USA), washed, and then reprobed with other antibodies as indicated.

RNA isolation and quantitative real-time RT-PCR. Total RNA was extracted with TRIzol (Invitrogen) and cDNA was synthesized using the cDNA synthesis kit (qScript™ cDNA Synthesis Kit; Quanta). SYBR Green fluorescent reagent and a MyiQ™2 two-color real-time detection system (Bio-Rad) were used for quantitative real-time RT-PCR. The relative amount of mRNA was calculated by the comparative threshold cycle method with *β–actin* as a control. The amplification efficiencies of all the primers were estimated by classical calibration dilution curve and slope calculation. For all housekeeping and target genes assessed, standard curves were evaluated on 10-fold serial dilutions of control bone

marrow derived macrophage cDNA to determine reaction efficiency. Specificity of primer pairs were evaluated by using both no-RT and water template control samples. Primer sequences are shown in the supplementary Table 1.

Flow cytometry analysis. Single-cell suspensions of thymi and secondary lymphoid organs were obtained by mincing the organs through a cell strainer dish. Primary cells or bone marrow derived macrophages were washed in FACS buffer (PBS/3%FBS), and stained according to standard procedures with the antibodies that specifically against each of the cell surface molecules including CD11b, CD11c, F4/80, MHC II, CD4, CD8, B220, IgM, CD206, Gr-1, FcεRIα (Biolegend, San Diego, CA, USA), and TLRs (eBioscience, San Diego, CA, USA). Intracellular staining of TNF-α (Biolegend, San Diego, CA, USA) was performed according to the protocol from eBioscience instructions. Flow cytometry was performed on a BD FACSCanto or Accuri C6 flow cytometery (BD Biosciences, San Diego, CA, USA). The data were analyzed using flowjo software excluding cell doublets. For analyzing apoptosis, the Annexin-V antibody (BD Biosciences) was used according to the manufacturer's protocol.

Histology. Tissue samples were prepared by fixing tissue 24-48 hr in 10% neutral buffered Formalin (VWR, West Chester, PA, USA). Fixed joints were decalcified by treatment with Decalcifying solution (Thermo, Rockford, MA, USA) for 24 hr. Samples were then washed with PBS, dehydrated with a series of ethanol washes (50% ethanol, followed by 70% ethanol), and embedded in paraffin. Sections of 4 μm were stained with H&E or preceded to immunohistochemical staining. Representative sections from individual mice within groups of 5-10 mice were selected to illustrate the general state of each group's ankle joints. Antibodies were purchased from the following companies: anti-Myeloperoxidase and anti-Tryptase (abcam, Cambridge, MA, USA); anti-MAC3 (BD Biosciences, San Diego, CA, USA); and secondary anti-rat IgG or anti-rabbit IgG (Vector laboratories, Burlingame, CA, USA).

Pulse chase assay for IRE1α protein synthesis and degradation. Mouse embryonic fibroblasts (MEFs) (1×10^6) were cultured for 24 hours before adding the methionine/cysteine-free media with ^{35}S-Methionine/Cysteine (100 μci/ml). After 2-4 hours of culture, the supernatant was changed to normal media and samples were collect at different time intervals for the following immunoprecipitation assays with the anti-IRE1α antibody.

References:

Yang WL, Wang J, Chan CH, Lee SW, Campos AD, Lamothe B, Hur L, Grabiner BC, Lin X, Darnay BG, Lin HK (2009) The E3 ligase TRAF6 regulates Akt ubiquitination and activation. *Science* **325:** 1134-1138

Supplementary Figure Legends

Supplementary Table 1.

Sequences of all primers used in this study are shown in the Supplementary Table 1.

Supplementary Fig. 1. Purity of the samples from RA and OA patients. Adherent cells from patients fluids were collect and analyzed by flow cytometry, the percentage of CD11b^{+} single positive cells **(A)** or CD11b^{+}CD206^{+} double positive cells **(B)** from RA (n=3) or OA (n=3) patient samples is shown. **(C)** The patient information was summarized and RA patients were grouped by their disease phase (acute *vs* chronic). The average XBP-1s levels are indicated. Student *t-test* was used for the statistic analysis, *$p<0.05$, **$p<0.01$, ***$p<0.005$. Iso, isotype controls.

Supplementary Fig. 2. Characterization of IRE1α gene deletion in macrophages. **(A)** T cells (CD3^{+}), B cells (B220^{+}) and macrophage (F4/80^{+} CD11b^{+}) from the spleens of IRE1α conditional knockout

($IRE1\alpha^{flox/flox}$ $LysM\text{-}Cre^{+}$) mice and their littermate controls ($IRE1\alpha^{+/+}$ $LysM\text{-}Cre^{+}$) were sorted. IRE1α

protein expression levels were analyzed by western blotting (top panel) using β-actin as a loading control.

(B) Thioglycollated elicited macrophage (F4/80^{+} CD11b^{high}) were sorted from wild-type and mutant mice,

the IRE1α protein expression was analyzed by western blotting as described in (A). **(C & D)** Peritoneal

cells were isolated from wild-type and mutant mice. The F4/80^{+} CD11b^{+} macrophages were sorted and

stimulated with TM (5μg/ml) for 16 hr. The mRNA levels of unspliced *XBP-1* and spliced *XBP-1* were

determined by semi-quantitative RT-PCR (C) or quantitative real-time RT-PCR (D).

Supplementary Fig. 3. The expression of CXCR2, CCR9, CD16 and CD5aR in myeloid cells from

the wild-type and *IRE1$\alpha^{f/f}$ LysM-Cre^{+}* mice. Wild-type and mutant mice were injected (I.P) with 150μl

K/BxN serum, 6 days after injection, macrophage (CD11b^{+}F4/80^{+}), neutrophils (CD11b^{+}Gr-1^{+}) and mast

cells (CD117^{+}FcεRIα^{+}) from peritoneal cavity, spleen and peripheral blood were collected for flow

cytometry analysis, representative data from independent experiments was shown. Solid lines indicate

wild-type (WT), dotted lines indicate knockout (KO) cells.

Supplementary Fig. 4. Analysis of macrophages in the wild-type and *IRE1$\alpha^{f/f}$ LysM-Cre^{+}* mice. **(A)**

Cells from the spleen (Spl, left panels) and peripheral lymph nodes (pLN, right panels) of *IRE1$\alpha^{f/f}$ LysM-*

Cre^{-} and *IRE1$\alpha^{f/f}$ LysM-Cre^{+}* mice were isolated. The macrophages were characterized by their cell

surface expression of CD11b and F4/80. **(B)** The bone marrow-derived macrophages from *IRE1$\alpha^{f/f}$ LysM-*

Cre^{-} and *IRE1$\alpha^{f/f}$ LysM-Cre^{+}* mice were analyzed for their cell surface expression of CD11b, F4/80, MHC

II and CD11c.

Supplementary Fig. 5. The development of immune cells in *IRE1α* conditional knockout mice. (A &

B) Thymocytes were isolated from the wild-type and *IRE1$\alpha^{f/f}$ LysM-Cre^{+}* mice and stained with

fluorescence-conjugated antibodies against CD4, CD8, CD25 and CD44. Cells were then analyzed for their expression of CD4 and CD8 (A). The CD4 and CD8 double negative cells were gated and their expression levels of CD44 and CD25 were analyzed (B). **(C-E & G)** Cells from the spleens of the wild-type and *IRE1α^{f/f} LysM-Cre^+* mice were isolated and stained with antibodies against each cell surface markers as indicated and analyzed by flow cytometry. The percentages of CD4 and CD8-positive cells are shown (C, left panels). The expression levels of CD44 and CD62L of the gated CD4^+ (C, middle panels) or CD8^+ T cells were analyzed (C, right panels). CD4^+ T cells from thymus or spleen were gated and the percentages of Tregs were determined by intracellular staining of FoxP3 and their cell surface expression of CD25 (**D**). The percentages of NK and NKT cells (**E**) were analyzed by NK1.1 and CD3 expression. DC subsets were analyzed by CD11c expression (**F**). **(G)** Bone marrow cells were isolated and the development of B cells was analyzed with anti-B220 and anti-IgM antibodies.

Supplementary Fig. 6. TLRs expression and apoptosis analysis of macrophages from wild-type and *IRE1α^{f/f}LysM-Cre^+* mice. (**A**) Bone marrow-derived macrophages from wild-type and mutant mice were stimulated with LPS (100 ng/ml), Pam3 (100 ng/ml), or poly(I:C) (10 μg/ml) for 24hr. The apoptotic subset of F4/80^+ CD11b^+ cells was analyzed by by Annexin V and PI staining. (**B**) The bone marrow-derived macrophages from *IRE1α^{f/f}LysM-Cre^-* and *IRE1α^{f/f}LysM-Cre^+* mice were analyzed for their expression of TLR2, TLR3 and TLR4 using specific antibodies or isotype controls (iso).

Supplementary Fig. 7. Characterization of neutrophils in *IRE1α*-deficient mice. (**A**) The percentage of spleen neutrophils (CD11b^+ Gr-1^+) and mast cells (CD117^+FcεR^+) in the spleens from wild-type and mutant mice are shown. (**B & C**) Anti-GPI serum (200μl/mouse) was intraperitoneally injected into wild-type and mutant mice. At 16 hr after the injection, peritoneal cavity cells were isolated. The absolute cell number (B) and distribution of neutrophils (CD11b^+Gr-1^+) were measured by flow cytometry (C). (**D**)

The isolated cells were further stimulated *in vitro* with LPS (1 μg/ml) for 3hr, TNF-α secretion was measured by flow cytometry. Representative images are shown. The percentages represent data from three pairs of mice. Student *t-test* was used for the statistic analysis, *p<0.05, **p<0.01, ***p<0.005.

Supplementary Fig. 8. Analysis of IRE1α activation in macrophages induced by TNF-α. (A & B) Bone marrow derived macrophages from ERAI mice were stimulated with LPS (100 ng/ml), Pam3 (100 ng/ml), polyI:C (10 μg/ml), TNF-α (20 ng/ml), or TM (5 μg/ml) for indicated time intervals. The GPF expression level (A) and mean fluorescence intensity (B) was measured by flow cytometry. **(C)** RAW264.7 (Mouse leukaemic monocyte macrophage cell line) cells were stimulated TNF-α (20 ng/ml) for the indicated time. The activation of IRE1α (phosph-IRE1α) was determined by phos-tag gel assay.

Supplementary Fig. 9. Reconstitution of IRE1α functions in the *IRE1α*–null cells with IRE1α mutants or with XBP-1s. WT and *IRE1α*-null MEFs were infected with control adenovirus or with that expresses IRE1α or it mutant (kinase-negative mutant, KM; RNase-negative mutant, RM) **(A)** or with XBP-1s **(B).** Cells were cultured for three days, re-plated onto 6-well plates and cultured in fresh media. Infected cells were then stimulated with or without LPS for 4 hours and the mRNA levels of IL-6 were determined by quantitative real-time PCR. Error bars represent data from a tri-placated study and the representative data from three experiments are shown.

Supplementary Fig. 10. Analysis of the regulated IRE1-dependent decay (RIDD) upon TLR response. Bone marrow-derived macrophages from wild-type and IRE1α mutant mice were stimulated with LPS (100ng/ml), Pam3 (100ng/ml), or polyI:C (10μg/ml) for 6h. The mRNA levels of RIDD genes (*Blos1*, *Hgna*t, *Pmp22*, *Scara3*, *Col6* and *PdgfR*) were determined by quantitative real-time RT-PCR

(qPCR). Error bars represent the SDs in qPCR replicates; representative data from two independent experiments are shown.

Supplementary Fig. 11. Analysis of ER stress signaling in the response to LPS. (A) Wild-type and *IRE1α*-null BMMs were stimulated with LPS (1 µg/ml) for 30 minutes or 24 hr, the levels of activated JNK (phosph-JNK) (top panel), total JNK (2nd panel), phosph-p38 (3rd panel), phosph-ERK1/2 (4th panel), and total Erk1/2 (5th panel) were analyzed by western blotting using specific antibodies. Tubulin level was determined as a loading control (bottom panel). The gene targeting of IRE1α in cells were also confirmed by western blotting (6th panel). **(B)** The levels of ER stress related proteins, including IRE1α, phosph-EIF2α, ATF6, and cleaved ATF6, were analyzed by western blotting.

Supplementary Fig. 12. Activation of IRE1α in MEFs under the stimulation of LPS. Wild-type and *TRAF6*-null MEF cells were stimulated with LPS (100ng/ml) for 16hr. The levels of spliced *XBP-1* mRNA were measured by quantitative real-time RT-PCR.

Supplementary Fig. 13. Glucose or serum regulates the interaction between PP2A and IRE1α. (A) Wild-type and *TRAF6* knockout MEF cells were cultured with glucose/serum-free media or normal media for 4 hours. Binging of PP2A to IRE1α was determined by immunoprecipitation with the anti-PP2A antibody (top panel). The expression levels of PP2A, IRE1α and TRAF6 in whole cell lysates were determined by western blotting analysis. **(B)** The intensities of IRE1α bands that interacted with PP2A were quantified. The relative band intensities are shown.

Supplementary Fig. 14. Analysis of IRE1α protein stability in cells upon LPS stimulation. (A) RAW cells were treated with 100 µg/ml cycloheximide (CHX) for the indicated time intervals in the presence or absence of LPS (1µg/ml). The protein levels of IRE1α (top panel) and tubulin (bottom panel) in the

lysates of treated cells were examined by western blotting analysis. **(B)** RAW cells were pulsed with ^{35}S-methionine for 4 hour. At the different time intervals indicated, LPS (1μg/ml) was added into the cell culture media. The IRE1α protein levels were measured by immunoprecipitation with the anti-IRE1α antibody. **(C & D)** RAW cells were stimulated with LPS for the indicated time points. (C) The IRE1α protein levels were detected by western blotting (top panel) using β-Actin as a control (bottom panel). (D) The band densities was quantified and normalized against the loading control β-Actin. Representitive data from three independent experiments are shown. **(E & F)** ^{35}S-methionine pulse chase analysis to measure the synthesis and degradation of IRE1α protein in MEF cells. Wild-type and *TRAF6*- null MEF cells were pulsed with ^{35}S-methionine media for 2 hours, and then the media was replaced with normal media. The samples were collected at the different time intervals indicated. The IRE1α protein levels were measured by immunoprecipitation with the anti-IRE1α antibody. The relative band intensities are shown in **(F)**.

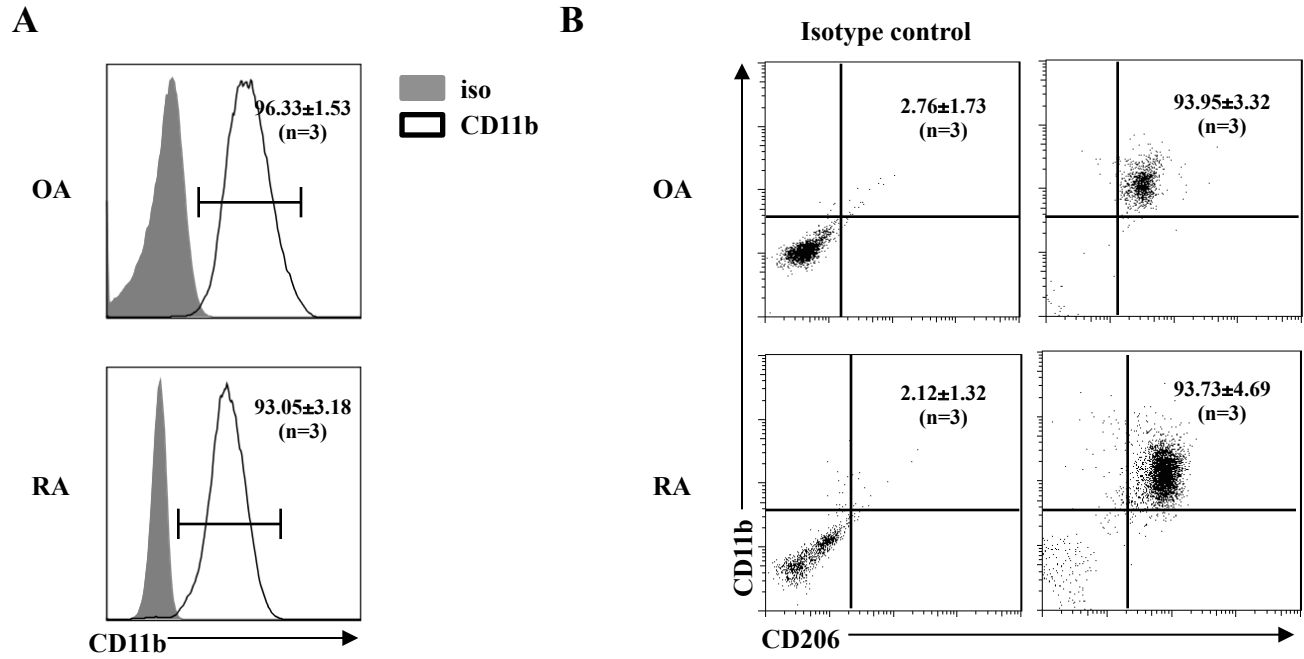**Supplementary Fig. 15. Expression level of PP2A in wild-type and *TRAF6*-null MEFs.** Cell lysates of wild-type and TRAF6 knockout MEFs were subjected to western blotting analysis of PP2A protein expression levels (top panel). *TRAF6* gene targeting in the MEFs was confirmed (middle panel). Actin levels were determined as loading controls (bottom panel).

Supplementary Table 1. Primers used in this study.

	Gene	Forward	Reverse
RT-PCR	Xbp1	ACACGCTTGGGAATGGACAC	CCATGGGAAGATGTTCTGGG
Q-PCR	IRE1α	GGGTTGCTGTCGTGCCTCGAG	TGGGGGCCTTCCAGCAAAGGA
	Xbp-1	ACACGCTTGGGAATGGACAC	CCATGGGAAGATGTTCTGGG
	Xbp-1s	GAGTCCGCAGCAGGTG	GTGTCAGAGTCCATGGGA
	IL-6	ACCTGTCTATACCACTTCACAAGT	TCTGCAAGTGCATCATCGTTGTTC
	IL1-β	CAACCAACAAGTGATATTCTCCATG	GATCCACACTCTCCAGCTGCA
	TNF-α	CCAGACCCTCACACTCAGATC	AGTTGGTTGTCTTTGAGATCCATG
	ISG15	AGCGGAACAAGTCACGAAGAC	TGGGGCTTTAGGCCATACTC
	Rantes	GCCTACCTCTCCCTCGCGCT	GGTTGGCACACACTTGGCGG
	IFN-β	TCCAGCTCCAAGAAAGGACG	GCATCTTCTCCGTCATCTCC

Supplemental Figure 1

A

OA

96.33±1.53 (n=3)

iso
CD11b

RA

93.05±3.18 (n=3)

CD11b

B

Isotype control

OA

2.76±1.73 (n=3)

93.95±3.32 (n=3)

RA

2.12±1.32 (n=3)

93.73±4.69 (n=3)

CD11b

CD206

C

Diseases	Patient number	Gender (M/F)	Age	XBP-1s		
RA/acute	13	2/11	43±16	512±203	P>0.1	P<0.05
RA/chronic	8	1/7	51±18	487±195	P<0.05	
OA (all acute)	7	4/3	46±19	229±126		

Supplemental Figure 2

A

WT IRE1α⁻/⁻

CD3⁺ B220⁺ F4/80⁺CD11b⁺ CD3⁺ B220⁺ F4/80⁺CD11b⁺

IRE1α — wt
— mutant

Actin

B

WT IRE1α⁻/⁻

IRE1α — wt
— mutant

Actin

C

CTL IRE1α⁻/⁻

TM (hr) 0 6 0 6

Xbp-1u —
Xbp-1s —
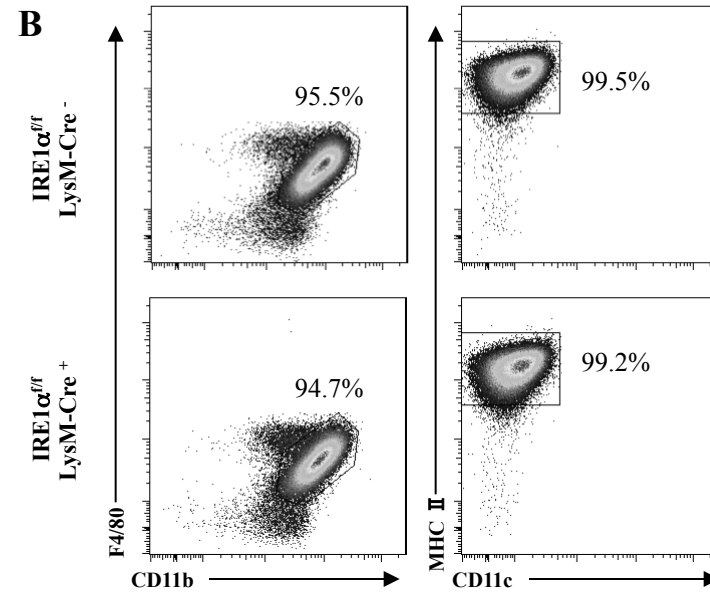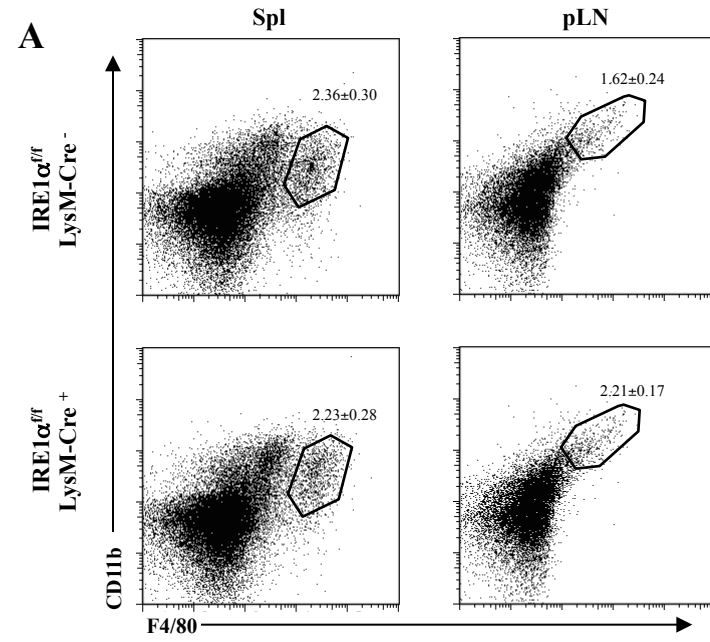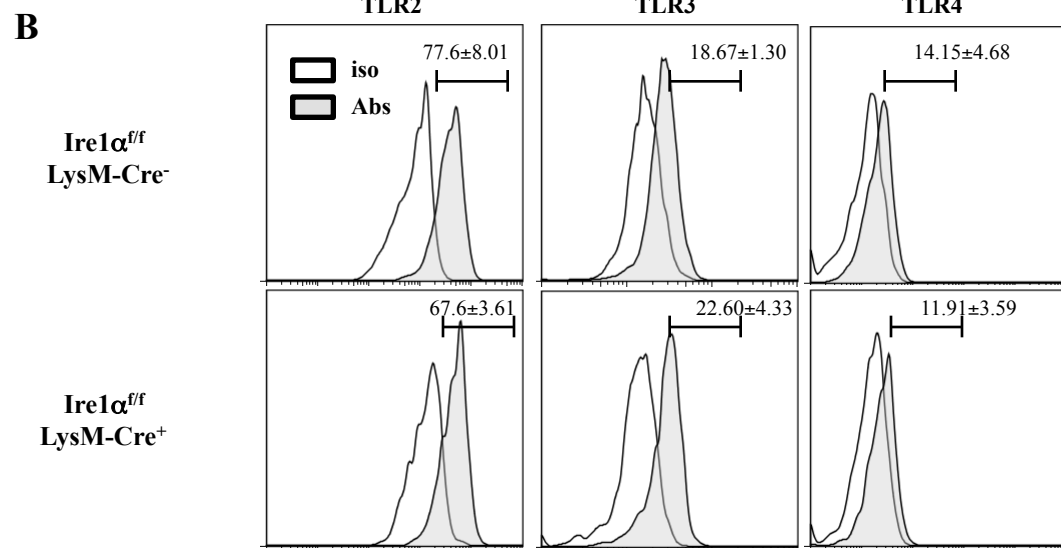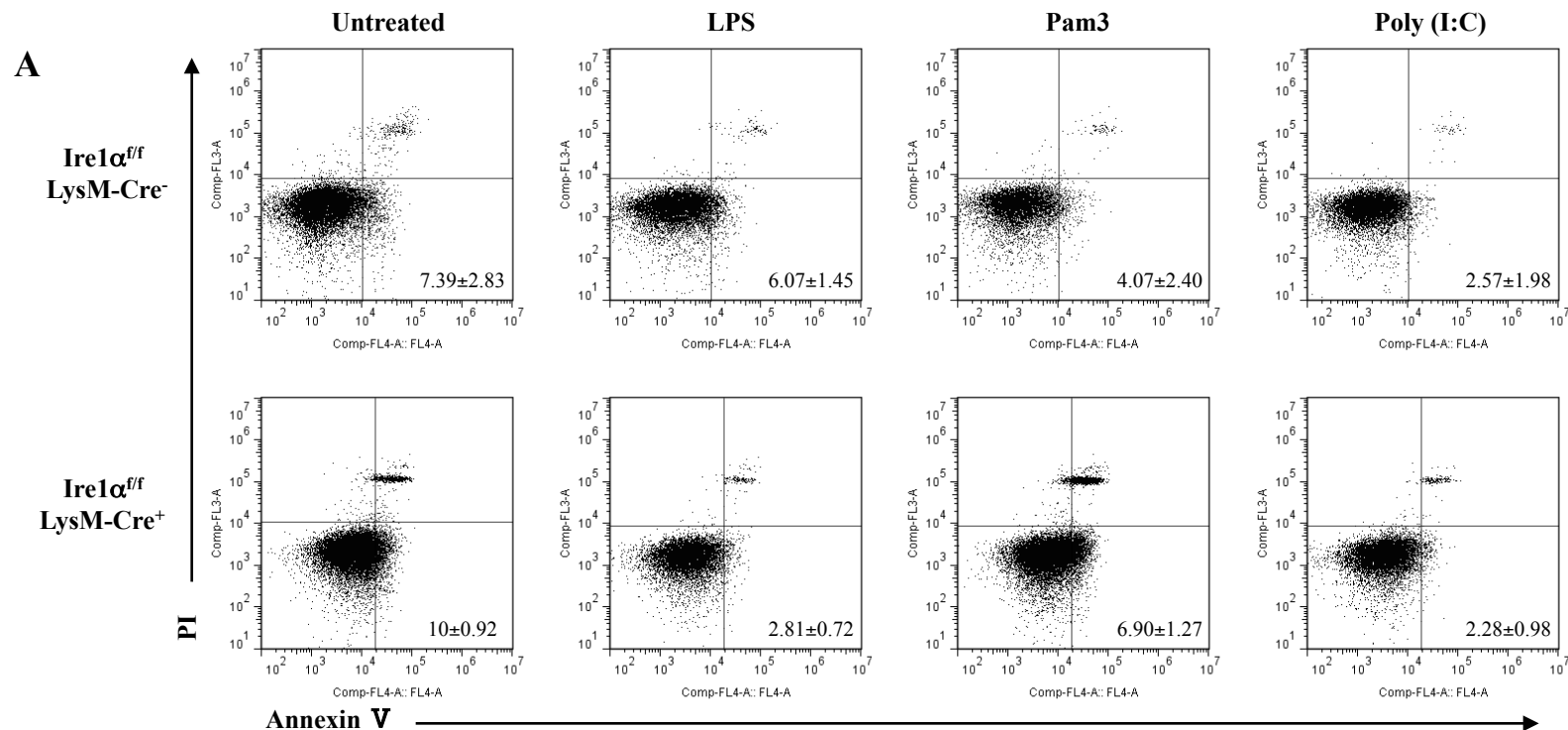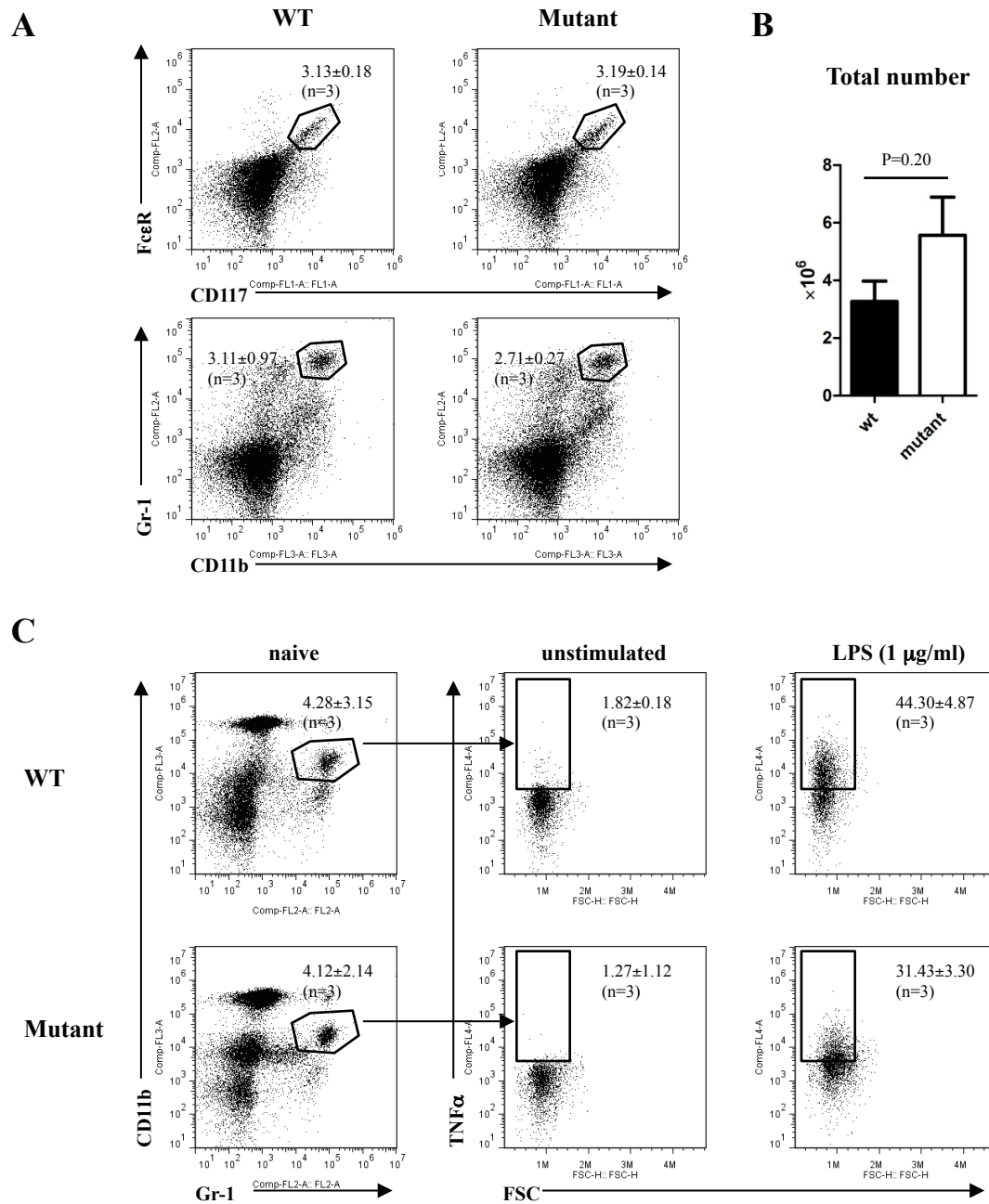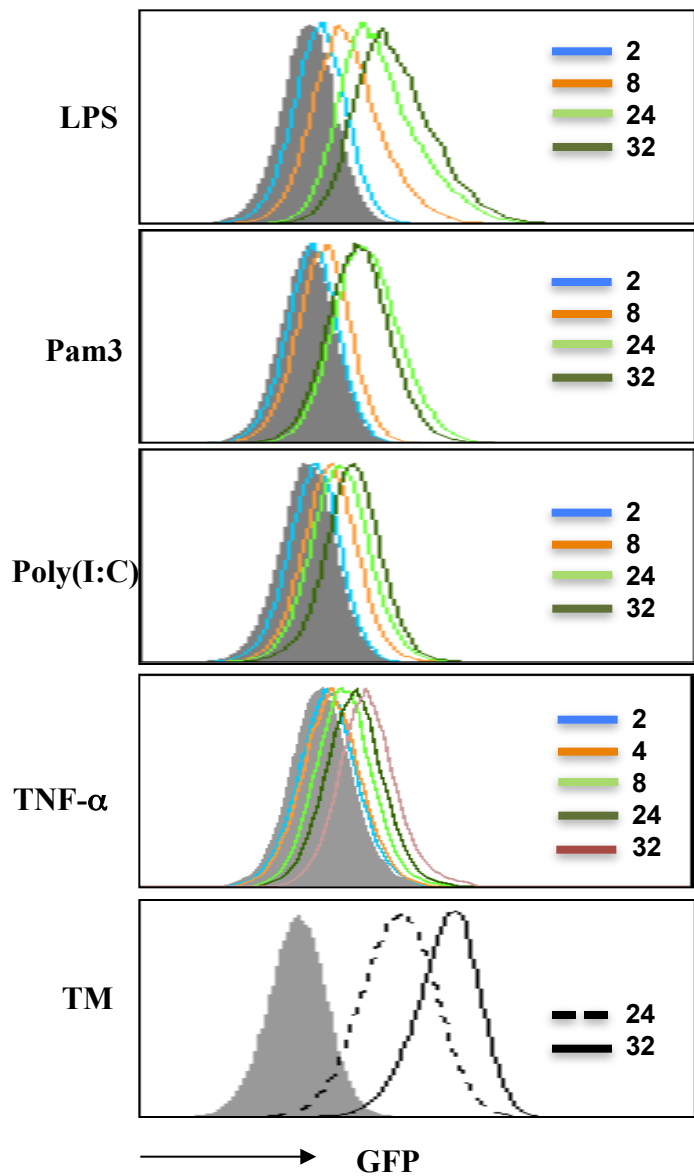
D
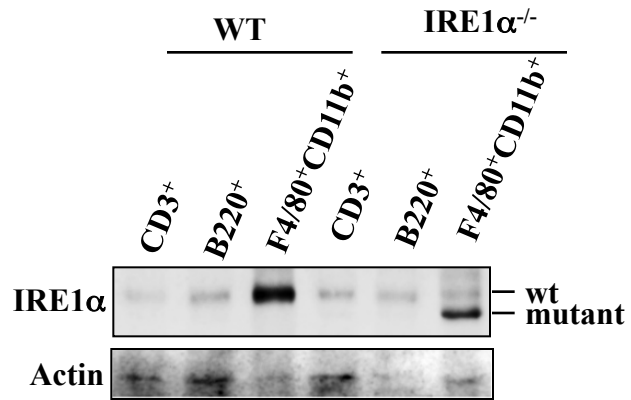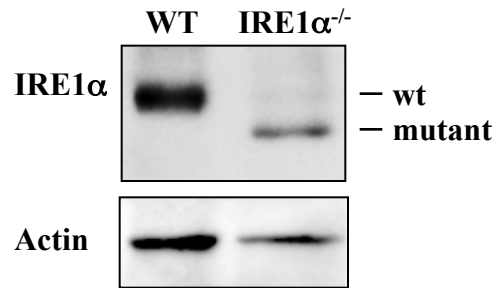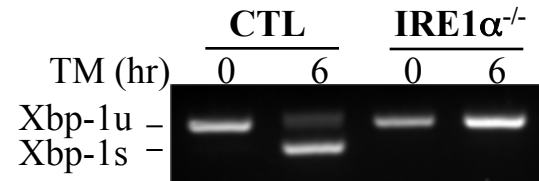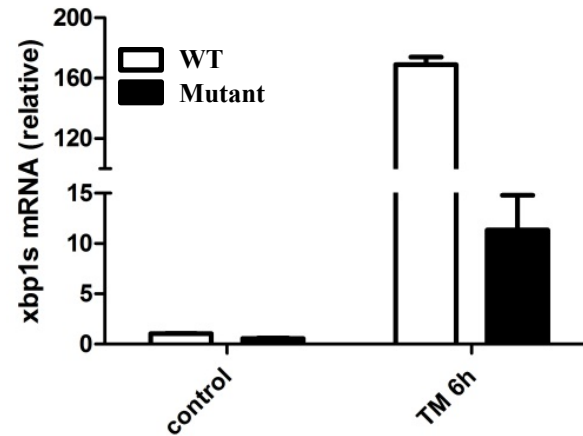
Supplemental Figure 3

Supplemental Figure 4

A

	Spl	pLN
IRE1α^{f/f} LysM-Cre^{-}	2.36±0.30	1.62±0.24
IRE1α^{f/f} LysM-Cre^{+}	2.23±0.28	2.21±0.17

CD11b (y-axis), F4/80 (x-axis)

B

IRE1α^{f/f} LysM-Cre^{-}: 95.5%, 99.5%

IRE1α^{f/f} LysM-Cre^{+}: 94.7%, 99.2%

F4/80 (y-axis), CD11b (x-axis); MHC II (y-axis), CD11c (x-axis)

Supplemental Figure 5

A

Thymus

CTL

6.10±0.76   87.97±0.91

2.30±0.09   1.68±0.17

IRE1α $^{-/-}$

6.38±1.31   87.07±2.14

2.64±0.43   1.91±0.34

CD4 / CD8

B

Thymus DN

9.23±1.36   9.18±2.68

32.07±2.08   39.73±0.31

8.74±0.87   6.84±1.78

33.70±2.62   41.87±1.80

CD44 / CD25

C

Spleen

15.37±1.51

8.40±1.46

14.50±1.11

8.62±0.44

CD4 / CD8

Spleen CD4 T

18.03±5.60   5.95±0.60

27.87±2.80   51.17±5.50

21.37±3.96   5.71±0.43

30.33±5.60   42.60±9.10

CD44 / CD62L

Spleen CD8 T

8.45±1.66   15.63±1.55

20.63±0.58   55.30±3.29

8.99±0.65   13.80±4.17

27.27±7.39   49.97±3.93

D

Thymus CD4

CTL

2.12±0.13

IRE1α $^{-/-}$

2.05±0.23

FoxP3 / CD25

Spleen CD4 T

8.35±0.50

8.58±0.37

E

Spleen

2.59±0.28

3.04±0.24

1.11±0.49

1.44±0.32

CD3 / NK1.1

F

Spleen

3.21±0.16   1.32±0.27

3.49±0.13   1.33±0.13

CD11c / B220

G

BM

5.50±0.57

22.47±2.90   9.43±1.45

5.55±0.35

20.10±2.69   8.01±1.21

B220 / IgM

Supplemental Figure 6

A

	Untreated	LPS	Pam3	Poly (I:C)

Ire1α[f/f] LysM-Cre[-]

Ire1α[f/f] LysM-Cre[+]

PI

Annexin V

B

TLR2   TLR3   TLR4

Ire1α[f/f] LysM-Cre[-]

Ire1α[f/f] LysM-Cre[+]
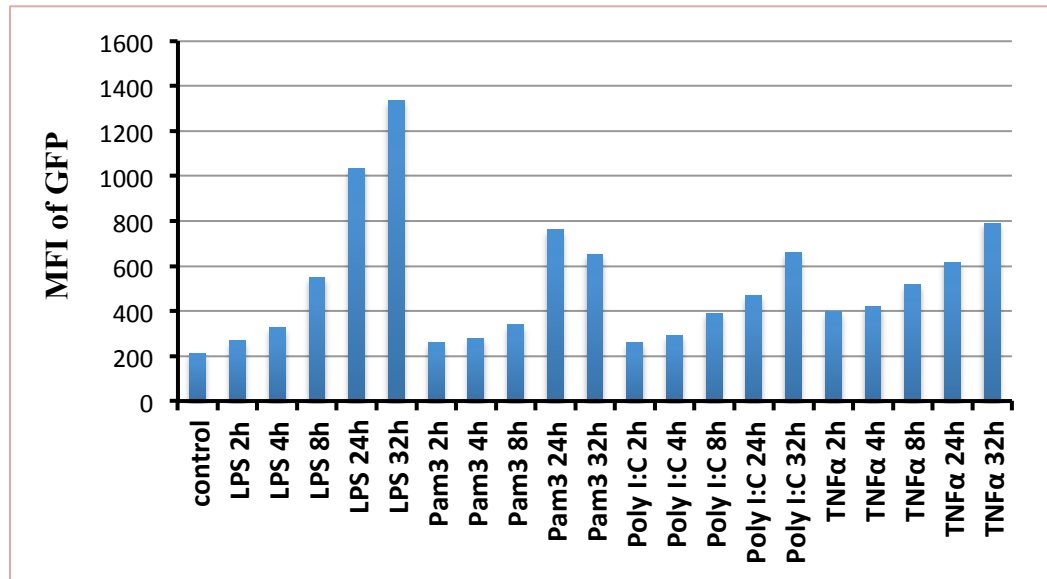
Supplemental Figure 7

A

B

Total number

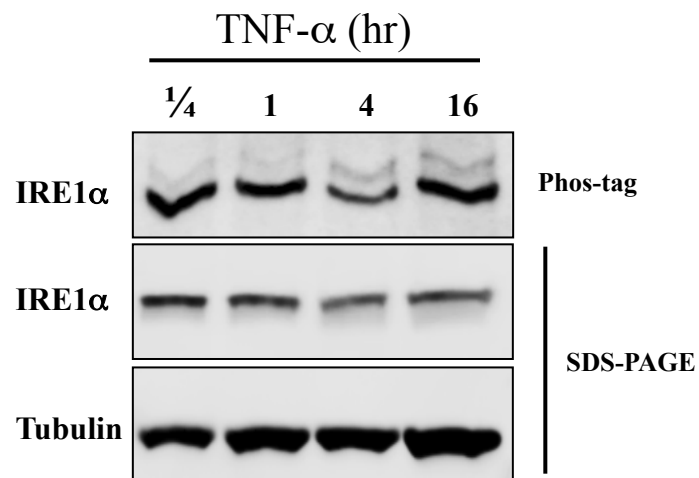**C**

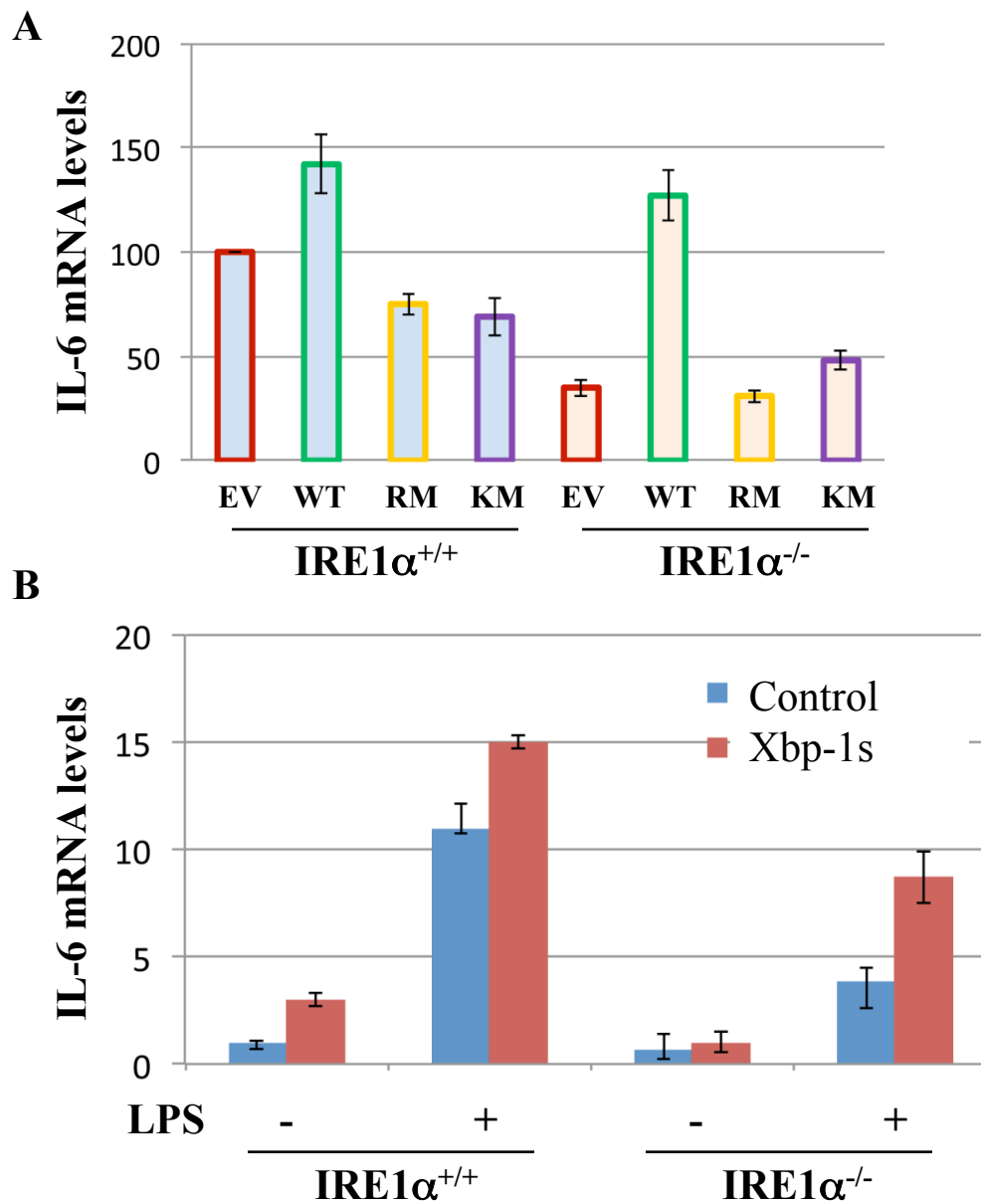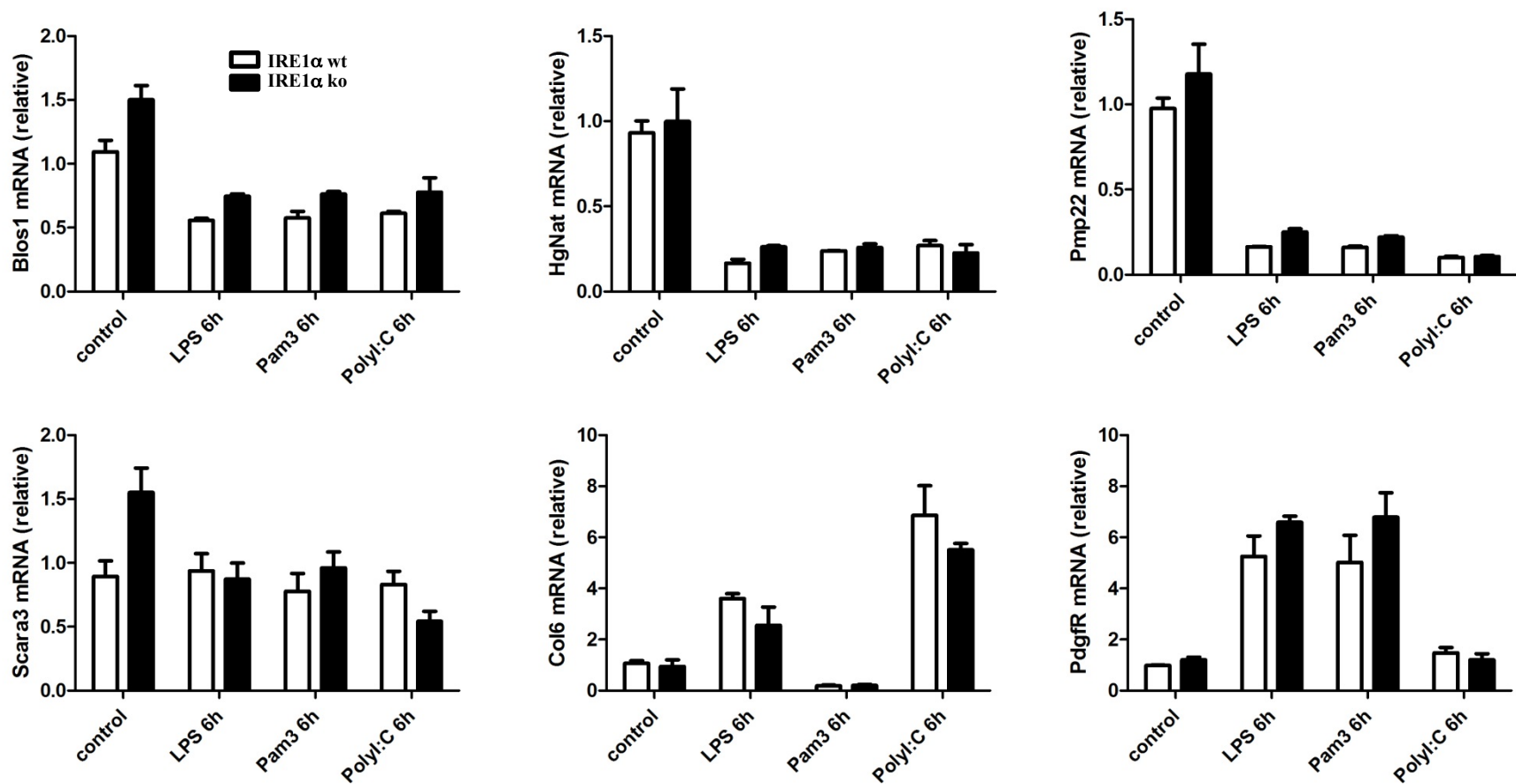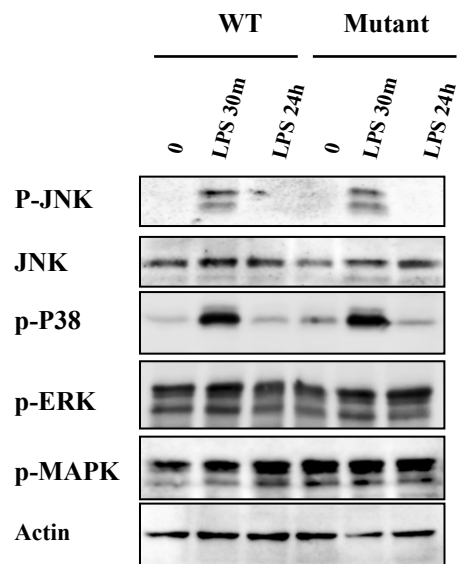# Supplemental Figure 8

A

B

C

Supplemental Figure 9
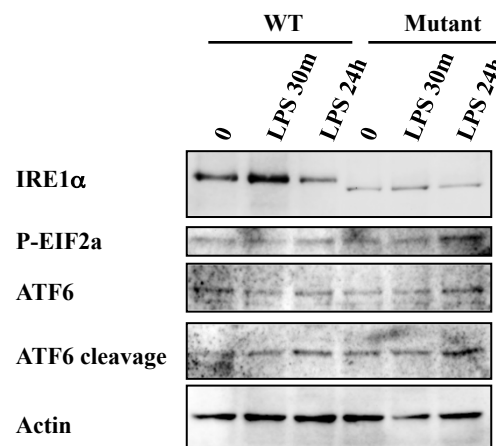
A

B

Supplemental Figure 10

Supplemental Figure 11
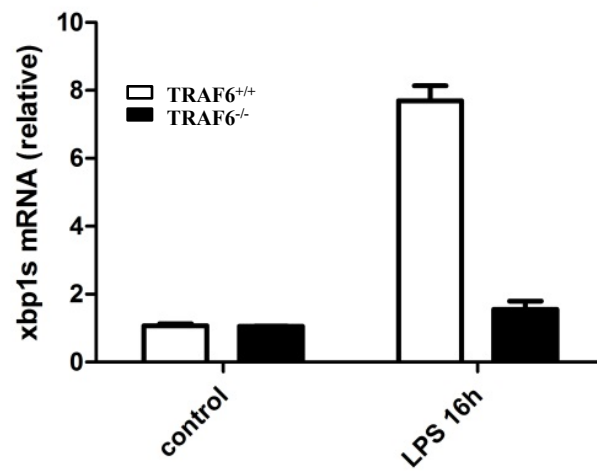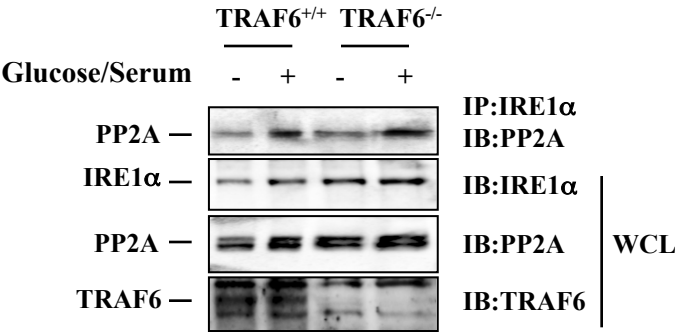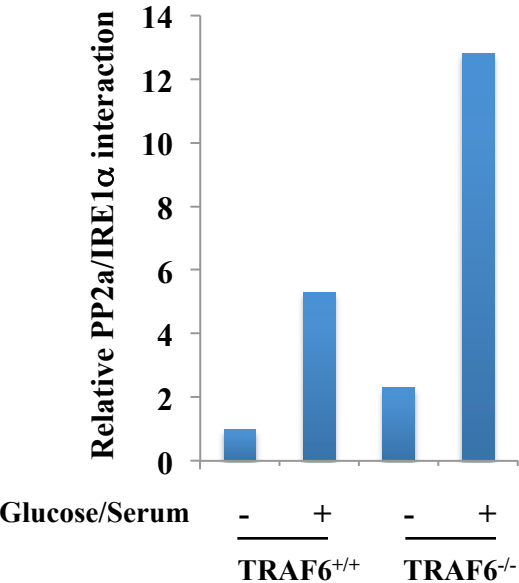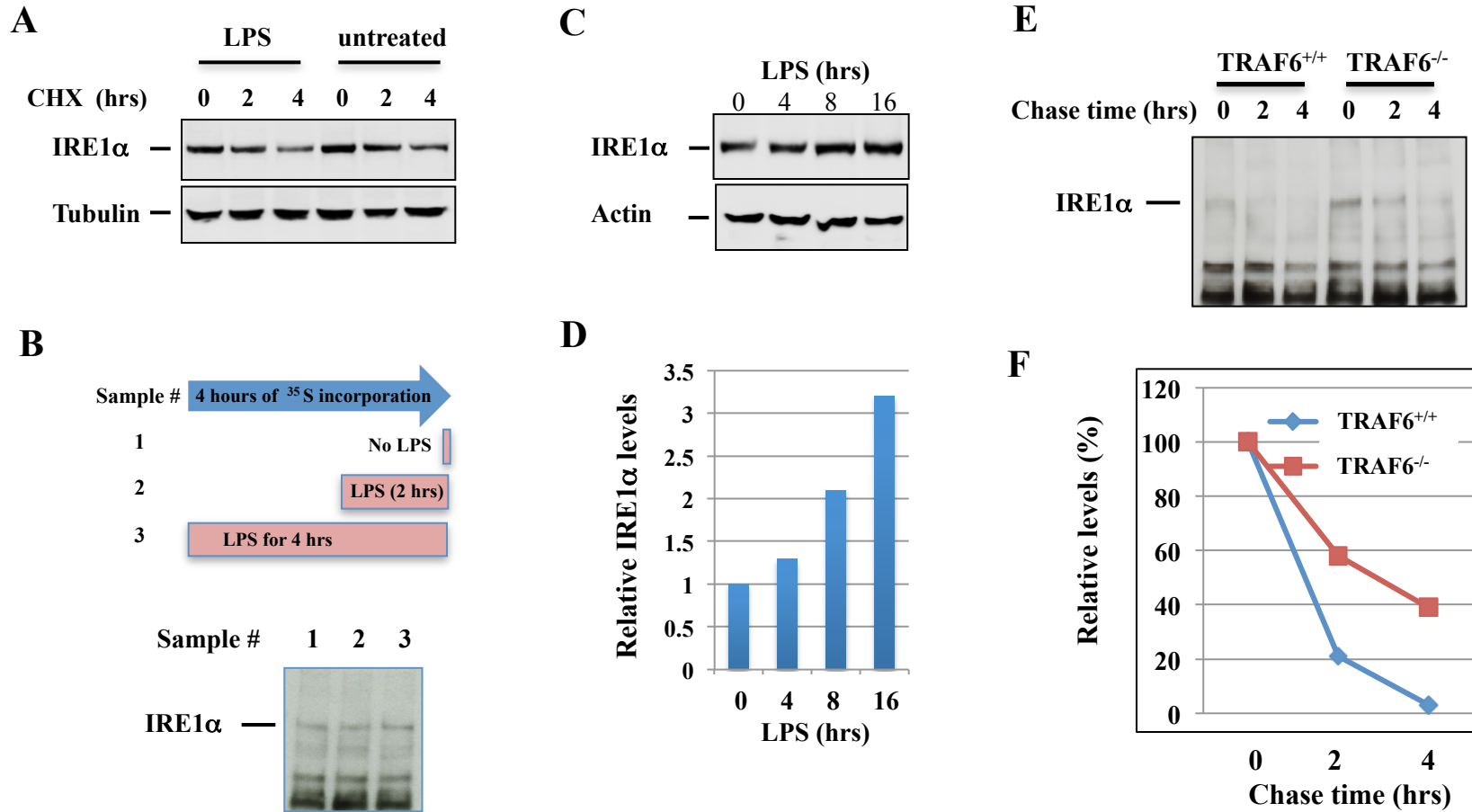
A

B

Supplemental Figure 12

Supplemental Figure 13

A

B

Supplemental Figure 14

A

LPS   untreated

CHX (hrs)   0 2 4   0 2 4

IRE1α —

Tubulin —

B

Sample #   4 hours of ^{35}S incorporation

1   No LPS

2   LPS (2 hrs)

3   LPS for 4 hrs

Sample #   1   2   3

IRE1α —

C

LPS (hrs)

0   4   8   16

IRE1α —

Actin —

D

E

TRAF6$^{+/+}$ TRAF6$^{-/-}$

Chase time (hrs)   0 2 4   0 2 4

IRE1α —

F

Supplemental Figure 15